arXiv:1703.03271v1 [nlin.SI] 9 Mar 2017

Coble's group and the integrability of the Gosset-Elte polytopes and tessellations

James Atkinson
08.03.17

Abstract. This paper considers the planar figure of a combinatorial polytope or tessellation identified by the Coxeter symbol $k_{i,j}$, inscribed in a conic, satisfying the geometric constraint that each octahedral cell has a centre. It is movable on account of some constraints being satisfied as a consequence of the others, and a close connection to the birational group found originally by Coble in the different context of invariants for sets of points in projective space, allows to specify precisely the subset of vertices that may be freely chosen. This gives a unified geometric view of certain integrable discrete systems in one, two and three dimensions. Making contact with previous geometric accounts in the case of three dimensions, it is shown how the figure also manifests as a configuration of circles generalising the Clifford lattices, and how it can be applied to construct the spatial point-line configurations called the Desargues maps.

1 Introduction

The six-point multi-ratio equation appears in the theory of integrable systems on a discrete domain with octahedral cells [1, 2, 3, 4, 5, 6]. It has the following geometric meaning, which has not been considered previously in this area.

Lemma 1.1. *If three lines meet a rationally parameterised conic at points corresponding to the three pairs of parameter values,*

$$\{x_{12}, x_{34}\}, \{x_{13}, x_{24}\}, \{x_{14}, x_{23}\}, \tag{1}$$

then the concurrence of the lines, Figure 1, is expressed analytically as

$$\frac{(x_{12}-x_{24})(x_{13}-x_{23})(x_{14}-x_{34})}{(x_{12}-x_{23})(x_{14}-x_{24})(x_{13}-x_{34})} = 1. \tag{2}$$

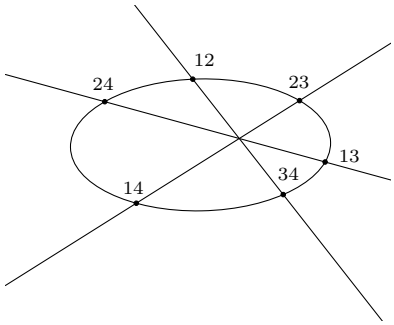

Figure 1: Concurrent secants of a conic.

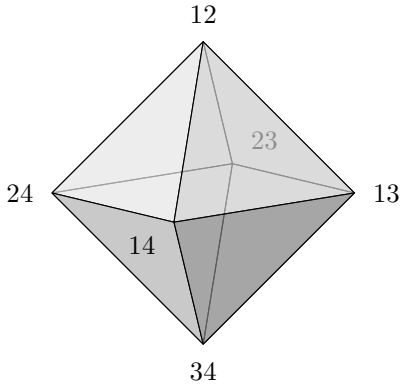

Figure 2: Octahedron with labelled vertices.

The calculation to verify this is straightforward, but a more affecting argument in the moduli space of quadratic polynomials is also provided in appendix A. Correspondence with the octahedron is shown in Figure 2.

The results of applying Lemma 1.1 are consistent with the observations of Adler [7] on other multi-ratio expressions. In those cases, there is an interesting connection between integrability and the generalisations of Pascal's theorem due to Möbius. The situation here is similar, but involves a different extension of Pascal's figure, described in Section 3.

The main result in Section 4 uses Lemma 1.1 to associate a combinatorial polytope or tessellation with Coxeter symbol $k_{i,j}$, that is inscribed in a conic, with a generalised form of Coble's birational group; the group is defined in Section 2. The points on the conic become points of a circle pattern when the conic is viewed as a model of the inversive plane. This generalises the previous geometric view of equation (2) established by Konopelchenko, Schief and King [8, 9], more precisely their circle-pattern is recovered in the case $k = 0$ here. The connection is explained in Section 6.

A planar incidence-geometry view of Coble's group has been established by Kajiwara, Masuda, Noumi, Ohta and Yamada [10], with particular attention to the solution in the case $1_{5,2}$ in terms of elliptic functions, and its equivariant extension to the $1_{6,2}$ case, that corresponds to the elliptic Painlevé equation [11]. The view established here treats uniformly all cases $k_{i,j}$, but turns out to be especially natural with-respect-to a simpler class of solutions that are rational; these are described in Section 5.

The Desargues maps introduced by Doliwa [5] are combinatorially rich point-line configurations that can be considered in $(\mathbb{P}^1)^M$ for any $M > 1$. In the commutative case, they are shown in Section 7 to separate into M independent systems each equivalent to case $k = 0$ of Coble's group, and this is applied to establish the natural determining-set for the configurations. Throughout this paper the projective space is defined over a field, the case of a skew-filed is discussed briefly at the end of Section 7.

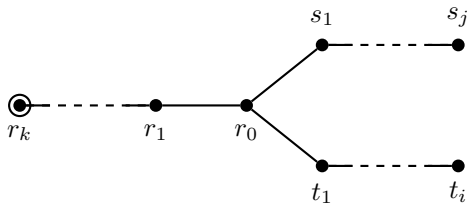

Figure 3: Coxeter graph with nodes corresponding to actions of Definition 2.1.

2 Birational group

The generalisation of Coble's group [12, 13] connecting it with equation (2) is as follows.

Definition 2.1 ([6])**.** *Let integers i, j be positive and k be non-negative. Introduce actions on the arrays of variables*

$$\begin{bmatrix} y_0 \\ y_1 \\ \vdots \\ y_k \end{bmatrix}, \quad \begin{bmatrix} y_{00} & y_{10} & \cdots & y_{i0} \\ y_{01} & y_{11} & \cdots & y_{i1} \\ \vdots & \vdots & & \vdots \\ y_{0j} & y_{1j} & \cdots & y_{ij} \end{bmatrix}, \tag{3}$$

as follows:

$$\begin{array}{rll} t_m: & y_{(m-1)n} \leftrightarrow y_{mn}, & m \in \{1,\dots,i\},\ n \in \{0,\dots,j\}, \\ s_n: & y_{m(n-1)} \leftrightarrow y_{mn}, & m \in \{0,\dots,i\},\ n \in \{1,\dots,j\}, \\ r_n: & y_{n-1} \leftrightarrow y_n, & n \in \{1,\dots,k\}, \\ r_0: & y_0 \leftrightarrow y_{00},\ y_{mn} \to \bar{y}_{mn}, & m \in \{1,\dots,i\},\ n \in \{1,\dots,j\}, \end{array} \tag{4}$$

where trivial actions are omitted, and $\bar{y}_{mn}$ is determined by the six-point multi-ratio equation imposed on variables

$$\{y_0, \bar{y}_{mn}\}, \{y_{0n}, y_{m0}\}, \{y_{00}, y_{mn}\}, \tag{5}$$

cf. Lemma 1.1, i.e.,

$$\frac{(y_0 - y_{m0})(y_{0n} - y_{mn})(y_{00} - \bar{y}_{mn})}{(y_0 - y_{mn})(y_{00} - y_{m0})(y_{0n} - \bar{y}_{mn})} = 1. \tag{6}$$

The generators (4) satisfy relations encoded in the Coxeter graph of Figure 3. Specifically, the group relations correspond to identities in the field of rational functions in the variables (3). The original group of Coble can be viewed as a partial integration of this one that is available if $k = 1$.

To give the description of this group afforded by Lemma 1.1, is the principal aim of this paper.

3 Extension of Pascal's hexagon

A suitable starting point is an elementary but intriguing extension to Pascal's figure of a hexagon inscribed in a conic.

Proposition 3.1. *Consider six points on a conic, C, labelled as follows:*

$$p_{\{1,3\}}, p_{\{2,4\}}, p_{\{1,5\}}, p_{\{2,3\}}, p_{\{1,4\}}, p_{\{2,5\}}. \tag{7}$$

Use $a+b$ to denote the line determined by two points, and $A \cap B$ to denote the point determined by two lines. By Pascal's theorem, the points

$$\begin{aligned} p_3 &:= (p_{\{1,4\}} + p_{\{2,5\}}) \cap (p_{\{2,4\}} + p_{\{1,5\}}), \\ p_4 &:= (p_{\{1,3\}} + p_{\{2,5\}}) \cap (p_{\{2,3\}} + p_{\{1,5\}}), \\ p_5 &:= (p_{\{1,3\}} + p_{\{2,4\}}) \cap (p_{\{2,3\}} + p_{\{1,4\}}), \end{aligned} \tag{8}$$

are collinear, determining a line π,

$$p_3 + p_4 = p_4 + p_5 = p_5 + p_3 =: \pi. \tag{9}$$

Add one further point to the figure, $p_{\{1,2\}}$, chosen freely on C. Lines connecting this point with the determining points of the Pascal line (8), intersect C at three further points, which we label as:

$$\begin{aligned} p_{\{4,5\}} &:= (p_{\{1,2\}} + p_3) \cap (C \setminus \{p_{\{1,2\}}\}), \\ p_{\{3,5\}} &:= (p_{\{1,2\}} + p_4) \cap (C \setminus \{p_{\{1,2\}}\}), \\ p_{\{3,4\}} &:= (p_{\{1,2\}} + p_5) \cap (C \setminus \{p_{\{1,2\}}\}). \end{aligned} \tag{10}$$

The following incidences then occur, determining two further points on π:

$$\begin{aligned} \pi \cap (p_{\{2,3\}} + p_{\{4,5\}}) = \pi \cap (p_{\{2,4\}} + p_{\{3,5\}}) = \pi \cap (p_{\{2,5\}} + p_{\{3,4\}}) =: p_1, \\ \pi \cap (p_{\{1,3\}} + p_{\{4,5\}}) = \pi \cap (p_{\{1,5\}} + p_{\{3,4\}}) = \pi \cap (p_{\{1,4\}} + p_{\{3,5\}}) =: p_2. \end{aligned} \tag{11}$$

See Figure 4.

Proof. Using again Pascal's theorem, we will show that

$$\pi \cap (p_{\{2,3\}} + p_{\{4,5\}}) = \pi \cap (p_{\{2,4\}} + p_{\{3,5\}}), \tag{12}$$

the other equalities in (11) are established the same way. Consider the inscribed hexagon whose vertices are, in consecutive order,

$$p_{\{1,2\}}, p_{\{3,5\}}, p_{\{2,4\}}, p_{\{1,5\}}, p_{\{2,3\}}, p_{\{4,5\}}. \tag{13}$$

Because of how $p_{\{1,2\}}$, $p_{\{4,5\}}$ and $p_{\{3,5\}}$ have been defined, we already know two of the three determining points for the Pascal line of this hexagon, they are

$$\begin{aligned} (p_{\{1,2\}} + p_{\{4,5\}}) \cap (p_{\{2,4\}} + p_{\{1,5\}}) = p_3, \\ (p_{\{1,2\}} + p_{\{3,5\}}) \cap (p_{\{2,3\}} + p_{\{1,5\}}) = p_4. \end{aligned} \tag{14}$$

Therefore, it is common with the original Pascal line (9), and the third determining point from hexagon (13) must also be somewhere on it, i.e.,

$$(p_{\{3,5\}} + p_{\{2,4\}}) \cap (p_{\{2,3\}} + p_{\{4,5\}}) \in \pi, \tag{15}$$

confirming (12). □

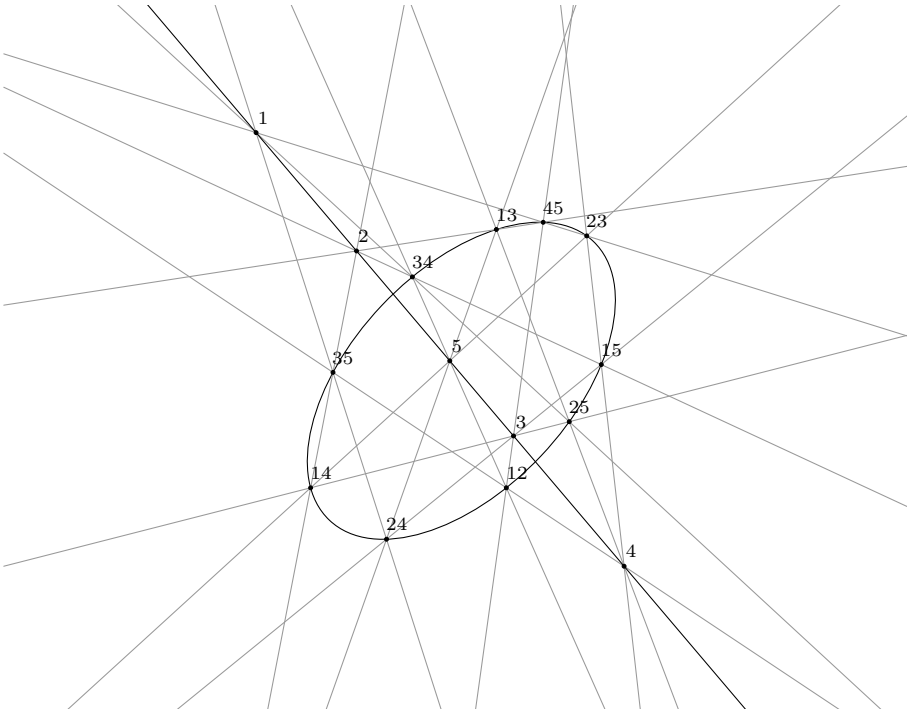

Figure 4: Illustration of Proposition 3.1, points $p_{\{\alpha,\beta\}}$ and p_γ are labelled as $\alpha\beta$ and γ respectively. The combinatorial symmetries of the figure correspond to free permutation of the five indices.

Instance $(k, i, j) = (0, 2, 1)$ of Definition 2.1 can be regarded as an analytic formulation of this proposition. Identify the elements of the arrays (3) with points on C as follows,

$$\left[\ p_{\{1,2\}}\ \right], \quad \begin{bmatrix} p_{\{1,3\}} & p_{\{1,4\}} & p_{\{1,5\}} \\ p_{\{2,3\}} & p_{\{2,4\}} & p_{\{2,5\}} \end{bmatrix}, \tag{16}$$

and the actions (4) with the permutations of indices that generate the combinatorial symmetries of the figure,

$$s_1 : 1 \leftrightarrow 2,\ r_0 : 2 \leftrightarrow 3,\ t_1 : 3 \leftrightarrow 4,\ t_2 : 4 \leftrightarrow 5. \tag{17}$$

The array on the right in (16) corresponds to the vertices of the original hexagon (7), and on the left, to the added point. The actions s_1, t_1 and t_2 generate the subgroup of combinatorial symmetries of the initial hexagon, and the action they induce, is simply to permute the rows and columns of the array on the right in (16). The index permutation $2 \leftrightarrow 3$ induces transposition of the first array elements, but it induces a set of geometric operations on entries corresponding to $p_{\{2,4\}}$ and $p_{\{2,5\}}$. The new points, $p_{\{3,4\}}$ and $p_{\{3,5\}}$, are determined from the given ones by (8) and (10). Performing these operations analytically using Lemma 1.1, by identifying points on C with corresponding values of a parameter, confirms the action of r_0 listed in Definition 2.1.

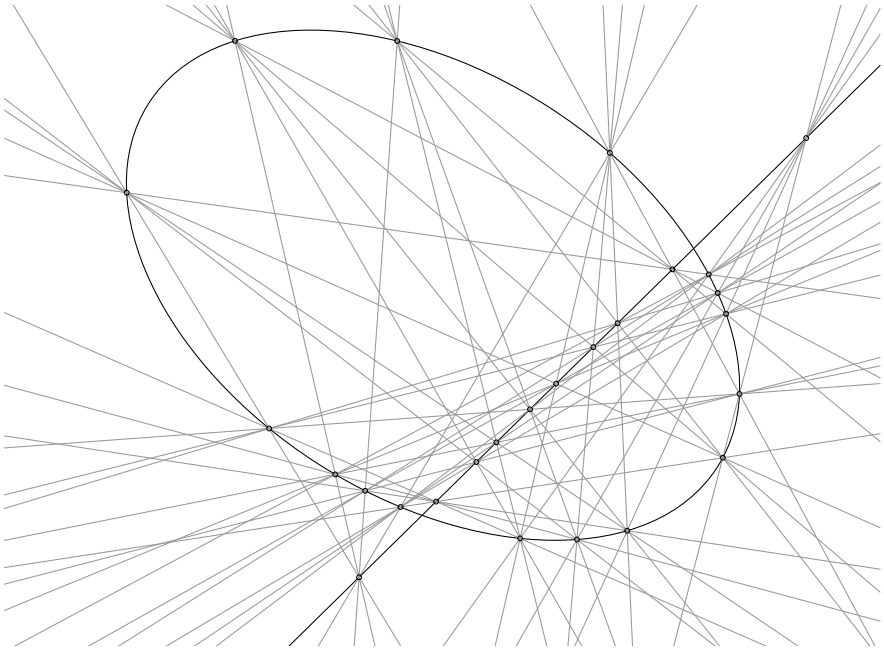

Figure 5: Example in the sequence of extensions of Pascal's hexagon corresponding to row three of Table 1.

This case illustrates the general situation. The arrays (3) correspond to the set of points on a conic from which a figure is determined, and elements of the group generated by (4) obtain the image of this determining-set under corresponding combinatorial symmetries of the figure. In the case just described the following can be checked by inspection.

Remark 3.2. With regard to the combinatorial symmetries of the figure, every vertex is contained in some image of the determining set, and the subgroup that fixes the determining-set point-wise, is trivial. This means the figure can be recovered from a determining-set using the group, and the group faithfully represents the combinatorial symmetries of the figure.

Loosely speaking, incrementing k iterates the procedure described in Proposition 3.1 by adding, at each step, a further freely chosen point on C, joining it to the previously marked points of π, and then adding more lines and points until the figure is symmetric. For example, Figure 5 shows the next in the sequence after Figure 4. After some iterations, this procedure fails to terminate. Some details of this sequence are given in Table 1.

On the other hand, larger values of i and j, due to the possible choices of three columns and two rows, or two columns and three rows, from the array on the right in (3), mean the determining-set involves multiple Pascal figures each with a different Pascal line. These lines form a configuration, the cases of finite configurations are listed in Table 2. The affine cases lead to configurations with a finite number of lines through each point and points on each line, but which are unbounded in number of points and lines.

	Points on C	Points on π	Pascal sub-figures
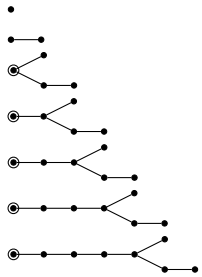	6 [2]	3 [2]	1
	10 [3]	5 [3]	10
	16 [5]	10 [4]	80
	27 [10]	27 [5]	720
	56 [27]	126 [6]	10080
	240 [126]	2160 [7]	483840

Table 1: Enumerative description of the finite figures related to case $(i, j) = (2, 1)$ of Definition 2.1. The first row corresponds to a single hexagon, and is a trivial case ($k = -1$) not included in Definition 2.1. The second row corresponds to Figure 4, and the third row to Figure 5. The number of lines (not including π) through each point is included in brackets.

	Points on C	Configuration Π
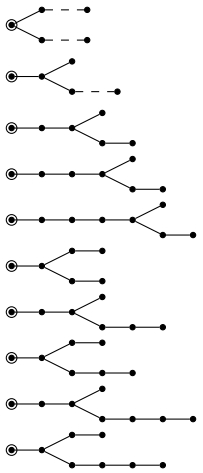	$\frac{(i+j+2)!}{(i+1)!(j+1)!}\left[\frac{i(i+1)j(j+1)}{4}\right]$	(p_{i+j-2}, q_5), $p = \frac{(i+j+2)!}{(i-1)!(j-1)!4!}$
	$2^{j+2}\left[\frac{(j+3)!}{(j-1)!4!}\right]$	(p_{j-1}, q_{10}), $p = \frac{2^{j-1}(j+3)!}{(j-1)!4!}$
	27 [10]	$(27_1, 1_{27})$
	56 [27]	$(126_1, 1_{126})$
	240 [126]	$(2160_1, 1_{2160})$
	72 [30]	$(270_2, 54_{10})$
	126 [60]	$(756_2, 56_{27})$
	576 [105]	$(7560_3, 2268_{10})$
	2160 [280]	$(60480_3, 6720_{27})$
	17280 [280]	$(604800_4, 241920_{10})$

Table 2: Enumerative description of finite figures related to Definition 2.1. The number of secants through each point on C is included in brackets. The Pascal lines form a configuration, Π. The notation (p_α, q_β) denotes a configuration of p points and q lines with α lines through each point and β points on each line; the constraint $p\alpha = q\beta$ corresponds to the total number of point-line incidences.

The combinatorial description of the general figure is obtained via a connection with certain uniform polytopes and tessellations.

4 Gosset-Elte figures inscribed in a conic

A combinatorial polytope in a projective space, is a point-line figure whose incidences correspond to the vertex-edge incidences of the polytope. Concerning the octahedron and its higher dimensional counterparts, namely the cross-polytopes,

we introduce the following terminology.

Definition 4.1. *A combinatorial cross-polytope with the property that the lines joining opposing vertices are all concurrent at a point, will be called a cross-polytope with a centre.*

This allows to describe Figure 1 as an octahedron with a centre inscribed in a conic. However, the edges are not marked, rather, the lines correspond to the axes, so it is a simpler skeleton from which the octahedron can be recovered. In the same way, Figures 4 and 5, are skeletons of a four-dimensional rectified simplex, and a five-dimensional demicube.

Indeed, the planar figures corresponding to Definition 2.1 for values of (i, j, k) satisfying $i + j + k + 1 \geq ijk - 1$, can each be described in terms of a corresponding figure from the Gosset-Elte family of uniform polytopes and tessellations. Coxeter [14, 15] introduced this family, giving a unified construction from the reflection group associated with Figure 3, and its members are subsequently identified by the corresponding (Coxeter) symbol $k_{i,j}$. Gosset and Elte separately discovered between them the exceptional cases, but the family also includes the infinite sequences of rectified simplexes corresponding to the case $k = 0$, the cross-polytopes when $i = j = 1$, and the demihypercubes when $i = k = 1$.

The connection to the birational group of Definition 2.1 is as follows.

Proposition 4.2. *View the entries of arrays (3) as parameters corresponding to points on a conic. For generic values, these points determine an inscribed combinatorial $k_{i,j}$-polytope or tessellation, constrained by the condition that all cross-polytope (or $k_{1,1}$) facets have a centre (Definition 4.1). The actions (4) give the image of the determining-set under combinatorial symmetries of the $k_{i,j}$-figure.*

Proof. The correspondence associating variables to vertices, and equations to octahedral cells of the $k_{i,j}$-polytopes and tessellations, was made previously in [6]. In outline, the discrete domain, like the corresponding $k_{i,j}$-figure, is a realisation of an incidence structure expressible in terms of cosets of the underlying Coxeter group. The proposition is therefore implied directly by Lemma 1.1, because it is clear that imposing that all octahedral cells have a centre, is equivalent to imposing that the cross-polytope facets do. The set of initial values for the discrete system corresponds to the determining set of the figure. The consistency of the initial-value-problem was established previously by reducing it to verifying the relations satisfied by the associated actions (4). That the figure in its entirety is determined, rather than some part of it, follows from the fact that the combinatorial symmetries are transitive on vertices of the $k_{i,j}$ figures. □

Because the vertices of the $k_{i,j}$-figure are confined to a conic, centres of all cross-polytope facets belonging to the same $k_{1,2}$ or $k_{2,1}$-facet, are themselves collinear. In the case of the rectified four-simplex ($0_{1,2}$-polytope) this is part of the content of Proposition 3.1, and the more general assertion is established by repeated application of this particular one.

Remark 4.3. The cross-polytope centres (Proposition 4.2) are therefore points of a planar point-line configuration (Π in Table 2), which is a realisation of the

incidence structure given by associating points with $k_{1,1}$-facets, and lines with the union of $k_{2,1}$ and $k_{1,2}$-facets, of the $k_{i,j}$-figure.

5 Ambient solution

An application of this geometric view of Coble's group (Proposition 4.2, Remark 4.3), is that we easily identify a special situation when *all* cross-polytope centres align, that suggests the birational group should linearise in terms of the associated geometric group on the conic.

To formulate this, we recall first the participating group. Denote the conic and the single Pascal line by C and π respectively. For any $a, b, e \in C \setminus \pi$, there exists a unique point $c \in C \setminus \pi$ such that the lines determined by the pairs $\{a, b\}$ and $\{c, e\}$, intersect π at the same point. The resulting mapping $(a, b) \mapsto c$ turns $C \setminus \pi$ into a group with identity e. In terms of corresponding parameters (x, y, z) for (a, b, c), we use the notation $z = x * y$ for the product, and x^{-1} for the inverse of x. This product is equivalent to either addition or multiplication in the field, depending on how π meets C.

Proposition 5.1. *The cross-polytope centres described in Proposition 4.2 lie on a common line π if, and only if, elements of the array (3) are such that*

$$y_{mn} = y_{00}^{-1} * y_{m0} * y_{0n}, \quad m \in \{1, \dots, i\}, n \in \{1, \dots, j\}. \tag{18}$$

This reduces the birational actions (4) to linear ones for the remaining variables:

$$\begin{array}{rll} t_m: & y_{(m-1)0} \leftrightarrow y_{m0}, & m \in \{2, \dots, i\}, \\ t_1: & y_{00} \leftrightarrow y_{10},\ y_{0n} \to y_{00}^{-1} * y_{10} * y_{0n}, & n \in \{1, \dots, j\}, \\ s_n: & y_{0(n-1)} \leftrightarrow y_{0n}, & n \in \{2, \dots, j\}, \\ s_1: & y_{00} \leftrightarrow y_{01},\ y_{m0} \to y_{00}^{-1} * y_{01} * y_{m0}, & m \in \{1, \dots, i\}, \\ r_n: & y_{n-1} \leftrightarrow y_n, & n \in \{1, \dots, k\}, \\ r_0: & y_0 \leftrightarrow y_{00}. & \end{array} \tag{19}$$

Proof. The intersection of lines determined by the two pairs $\{y_{mn}, y_{\alpha\beta}\}$ and $\{y_{m\beta}, y_{\alpha n}\}$ taken from the array on the right in (3), where $m \neq \alpha$ and $n \neq \beta$, is the centre of an octahedral cell. The condition for these centres to be on π can be expressed in terms of the geometric group on $C \setminus \pi$, as

$$y_{mn} * y_{\alpha\beta} = y_{m\beta} * y_{\alpha n}, \quad m, \alpha \in \{0, \dots, i\},\ n, \beta \in \{0, \dots, j\}. \tag{20}$$

The conditions (18) are clearly a subset of the conditions (20). That (18) implies (20) is established by substitution, relying on associativity of the group and therefore Pascal's theorem in geometric terms.

To verify that all octahedral centres are on π, it is sufficient to show that the actions (4) preserve the condition (18). For the actions $t_1, \dots, t_i, s_1, \dots, s_j$ this follows from the established equivalence between (18) and (20). For the action r_0 it follows from the concurrence of lines determined by the three pairs of points (5), which was the content of Lemma 1.1. For the remaining actions $r_1, \dots, r_k$ it is trivial. □

In the case $k_{1,2}$, corresponding to the sequence in Table 1, there is only a single Pascal line, so there is no loss of generality if (18) is assumed. The subgroup

associated with the $1_{5,2}$-tessellation is known to be linearised by substitution of elliptic functions, and Proposition 5.1 shows that rational functions are sufficient for the $5_{2,1}$-tessellation. Nevertheless, it determines an $\tilde{E}_8$ action on $\mathbb{P}^1 \times \mathbb{P}^1$ by equivariant extension to the case $5_{3,1}$. It would therefore be interesting to know where this fits in relation to the QRT maps [16] and classification of discrete Painlevé equations [11].

6 Associated circle patterns

If the projective plane over $\mathbb{C}$ is viewed as a four-dimensional real space, then a conic in the plane is seen as a quadric surface in the space. Three points on the conic correspond to points on the surface that are either on a line within the surface, or determine a plane that cuts it. In this way, the surface constitutes an inversive plane; each curve determined by a set of three points, corresponds to a circle.

Remark 6.1. The ambient notion of general-position for sets of points in an inversive plane, has the requirement that no four points be on the same circle. The corresponding requirement is absent in the projective setting.

In this model of the inversive plane, equation (2) is an analytic form of a geometric constraint established in [8, 9], that the four circles determined by sets of points

$$\{x_{12}, x_{23}, x_{13}\}, \{x_{23}, x_{34}, x_{24}\}, \{x_{13}, x_{34}, x_{14}\}, \{x_{12}, x_{24}, x_{14}\}, \tag{21}$$

are concurrent at a point. Or, equivalently, due to Clifford's four-circle theorem, that the circles determined by the sets

$$\{x_{12}, x_{13}, x_{14}\}, \{x_{12}, x_{23}, x_{24}\}, \{x_{13}, x_{23}, x_{34}\}, \{x_{14}, x_{24}, x_{34}\}, \tag{22}$$

are. The resulting figure of eight circles and eight points, is the C_4 pattern appearing first in Clifford's chain of theorems. By symmetry, the condition can be reduced to the equivalent one, that any three of the circles meet at a point. The sets of points (21) and (22) correspond to the eight faces of the octahedron. In summary, we have the following.

Corollary 6.2 (of Proposition 4.2)**.** *View the entries of arrays (3) as points in the inversive plane. In general position, these points determine a combinatorial $k_{i,j}$-polytope or tessellation, constrained by the condition that the vertices of each octahedral cell correspond to points of a C_4 circle pattern (see above). When the inversive plane is identified with $\mathbb{C} \cup \{\infty\}$, the actions (4) give the image of the determining-set under combinatorial symmetries of the $k_{i,j}$-figure.*

The statement of existence and movability of the circle patterns in the case $k = 0$ was given originally in relation to the integrability of equation (2) in [8], where it was shown to be an extension of the patterns in Clifford's chain. Longuet-Higgins [17] actually related Clifford's chain to the $1_{1,j}$-polytopes (demihypercubes), and added new examples to previously known configurations of points and hyperspheres in connection with the remaining (finite) list of $1_{i,j}$-polytopes. The patterns here are planar, so they have a different

$(6_2, 4_3)$	$(10_3, 10_3)$	$(15_4, 20_3)$	$(21_5, 35_3)$	$(28_6, 56_3)$
$(10_2, 5_4)$	$(20_3, 15_4)$	$(35_4, 35_4)$	$(56_5, 70_4)$	$(84_6, 126_4)$
$(15_2, 6_5)$	$(35_3, 21_5)$	$(70_4, 56_5)$	$(126_5, 126_5)$	$(210_6, 252_5)$
$(21_2, 7_6)$	$(56_3, 28_6)$	$(126_4, 84_6)$	$(252_5, 210_6)$	$(462_6, 462_6)$
$(28_2, 8_7)$	$(84_3, 36_7)$	$(210_4, 120_7)$	$(462_5, 330_7)$	$(924_6, 792_7)$

Table 3: Enumerative description of the first few of Doliwa's configurations associated with Coxeter symbol $0_{i,j}$. The balanced (10_3), corresponding to Coxeter symbol $0_{1,2}$, is Desargues' configuration.

nature, but they exist uniformly in relation to all of the $k_{i,j}$-polytopes and tessellations.

The mismatch between our and the Longuet-Higgins Coxeter symbol, is seen already in the case of the C_4 pattern described above. The two additional points are on the same footing as the original ones, and the eight taken together correspond to vertices of the four-dimensional cross-polytope, whereas the original constraint corresponds to the octahedron. This feature is related to Remark 6.1, however, a generalisation to higher dimension without this feature as been obtained [18], and it would be interesting to know if those patterns have a projective formulation.

Circle patterns for Riccati solutions of discrete Painlevé equations have been related to discrete analogues of holomorphic functions [19, 20]. The circle patterns here are instead associated with the general solution, but the hypergeometric solutions of the elliptic Painlevé equation [10] are also framed geometrically in terms of a conic.

7 Desargues maps

In terms of the Coxeter symbol, the Desargues maps of Doliwa [5, 21] in the fundamental region, are a combinatorial $0_{i,j}$-polytope satisfying the condition that vertices of all $0_{i,0}$-facets are collinear. It means some edges coalesce resulting in a point-line configuration; in summary we highlight the following.

Remark 7.1. At the core of the Desargues maps, is a point-line realisation of the incidence structure defined by vertices and $0_{i,0}$-facets of the $0_{i,j}$-polytope.

This is a (p_{j+1}, q_{i+2}), $p = (i+j+2)!/[(i+1)!(j+1)!]$, configuration, the first few cases are given in Table 3. Although they are both simplexes, we distinguish the $0_{0,j}$-facets from $0_{i,0}$ ones, which breaks the antipodal symmetry of the $0_{i,i}$-polytopes, or equivalently the Coxeter graph automorphism. There is a direct relationship between the Desargues maps whose image is in $(\mathbb{P}^1)^M$, $M > 1$, over a field, and the form of Coble's group in Definition 2.1, which leads to the following.

Proposition 7.2. *Freely choose a point in $(\mathbb{P}^1)^M$, $j+1$ lines through it, and $i+1$ additional points on each line. In general position, this is a determining-set for Doliwa's configuration associated with Coxeter symbol $0_{i,j}$ (Remark 7.1).*

Denote the first freely chosen point by y_0 and, for each $n \in \{0, \ldots, j\}$, denote the $i+1$ additional points on the n^{th} line passing through y_0, by $y_{0n}, \ldots, y_{in}$.

$(1_0, 0_5)$	$(5_1, 1_5)$	$(15_2, 6_5)$	$(35_3, 21_5)$	$(70_4, 56_5)$
$(5_1, 1_5)$	$(30_2, 12_5)$	$(105_3, 63_5)$	$(280_4, 224_5)$	$(630_5, 630_5)$
$(15_2, 6_5)$	$(105_3, 63_5)$	$(420_4, 336_5)$	$(1260_5, 1260_5)$	$(3150_6, 3780_5)$
$(35_3, 21_5)$	$(280_4, 224_5)$	$(1260_5, 1260_5)$	$(4200_6, 5040_5)$	$(11550_7, 16170_5)$
$(70_4, 56_5)$	$(630_5, 630_5)$	$(3150_6, 3780_5)$	$(11550_7, 16170_5)$	$(34650_8, 55440_5)$

Table 4: Enumerative description of the first few configurations associated with Coxeter symbol $0_{i,j}$ described in Remark 4.3

Then generators (4) in the case $k = 0$, acting diagonally on $(\mathbb{P}^1)^M$, give the image of this determining set under combinatorial symmetries of the configuration.

Proof. The main reason is understood in the case $i = j = 1$, $M = 2$; the case of the $(6_2, 4_3)$ configuration, which is the complete quadrilateral. If six elements of $(\mathbb{P}^1)^2$ are labeled by vertices of the octahedron, then imposing the four lines (21), is equivalent to imposing any two of the lines and the multi-ratio condition (2) on each coordinate separately. It was explained in [8] that this essentially goes back to Menalaus' theorem. It follows from this, that the diagonal actions described in the proposition preserve the collinearity assumed for the determining-set; it is trivial for all actions except r_0, and for this one it is sufficient to consider the case described.

Observe now (separately from the above) that the 0_{i0} sub-graph of generators (4), i.e., $r_0, t_1, \ldots, t_i$, freely permutes entries $y_0, y_{00}, y_{10}, \ldots, y_{i0}$ of arrays (3), so in accordance with the correspondence described in Proposition 4.2, these entries correspond to vertices of a $0_{i,0}$-facet. Also notice, that all rows of the array on the right in (3) are on the same footing, because the rows are themselves freely permuted by the actions $s_1, \ldots, s_j$. Therefore the rows of the array on the right in (3) correspond to vertices of $j + 1$ $0_{i,0}$-facets whose common vertex corresponds to y_0.

The second paragraph of the Proposition follows by combining these two observations. The first shows that the diagonal actions described determine a point-line figure in $(\mathbb{P}^1)^M$, and the second that it coincides with Doliwa's $0_{i,j}$ configuration.

It is clear the general configuration is determined by the group actions, because, first, all that is imposed is the linearity and multi-ratio constraints on each octahedral cell, which are both necessary. Second, that the whole configuration is obtained, and not some part of it, follows from the fact that the group of combinatorial symmetries of the $0_{i,j}$ polytope acts transitively on vertices. This establishes the first paragraph of the Proposition. □

This proposition shows that the Desargues maps whose image is in $(\mathbb{P}^1)^M$ over a field, decompose into M simpler independent systems, each equivalent to case $k = 0$ of Coble's group. The corresponding result for the skew field is likely to hold, because the consistency for Doliwa's configurations is encoded in Desargues' theorem, and not Pascal's [5, 9]. The circle patterns corresponding to the case $k = 0$ have also been generalised in this direction [18]. Given the view established by Lemma 1.1, it would therefore be interesting to know if this form of Coble's group can extend to the skew-field setting in the case $k > 0$.

In this regard, a basic question to shed some light, is to know the geometric origin of the consistency property underlying the movability of the point-line configurations Π of Remark 4.3. The first few cases associated to the Coxeter symbol $0_{i,j}$ are displayed Table 4 for comparison with Table 3.

The connection to the Desargues maps is not a geometric one. It is possible to see them as a special case of the circle patterns [9] in which all circles become lines, but they then appear in a restricted setting. However, Proposition 7.2 is equivalent to a symmetry of the actions (4) present when $k = 0$. A similar kind of symmetry is also present in the case $k = 1$; it is inferred from the integration that recovers Coble's group in its original form [6]. It is therefore an interesting question to understand the geometric origin of these symmetries in the context of Lemma 1.1.

Acknowledgements

I very grateful to Pavlos Kassotakis for our discussions on this topic.

A Proof of Lemma 1.1

There is an equivalence between identifying a polynomial of degree n with its set of factors, and the identification of a hyperplane in $\mathbb{P}^n$ by the set of points where it intersects the *rational normal curve*,

$$(a^n : a^{n-1}b : \ldots : ab^{n-1} : b^n), \quad (a : b) \in \mathbb{P}^1,$$

the order of the contact with the curve corresponds to multiplicity of the factor. We use this here in the case $n = 2$, when the curve is a conic, to verify Lemma 1.1.

In the polynomial context, the main observation is that:

Lemma A.1. *Equation (2) is the condition for linear dependence of the three quadratic polynomials,*

$$(x - x_{12})(x - x_{34}),\ (x - x_{13})(x - x_{24}),\ (x - x_{14})(x - x_{23}). \tag{23}$$

Proof. The equation (2) can be written differently as

$$\begin{vmatrix} x_{12}x_{34} & x_{12} + x_{34} & 1 \\ x_{13}x_{24} & x_{13} + x_{24} & 1 \\ x_{14}x_{23} & x_{14} + x_{23} & 1 \end{vmatrix} = 0, \tag{24}$$

which is the condition on polynomial coefficients for the linear dependence. □

Take the representation of $\mathbb{P}^2$ where *lines* and *points*, respectively, are represented by the *one* and *two* dimensional subspaces in the vector space of polynomials whose degree is less than or equal to two. This is dual to taking polynomial coefficients as projective coordinates. In this representation, the subspaces of polynomials defined by a shared root,

$$\langle ax - b, x(ax - b)\rangle, \quad (a : b) \in \mathbb{P}^1, \tag{25}$$

represent the points of a conic, and the subspaces of polynomials with a double root,

$$\langle (ax - b)^2\rangle, \tag{26}$$

represent its corresponding tangent lines. Distinct elements $(a:b),(c:d) \in \mathbb{P}^1$ determine a secant,

$$\langle ax-b, x(ax-b)\rangle \cap \langle cx-d, x(cx-d)\rangle = \langle (ax-b)(cx-d)\rangle. \qquad (27)$$

The linear dependence of polynomials (23) is concurrence of corresponding secant or tangent lines, and therefore Lemmas 1.1 and A.1 are equivalent.

One reason we verify Lemma 1.1 in this way, is due to the related form of Coble's group established in [22, 23]. That form involves the case $n = 3$ above, of concurrent planes passing through a twisted cubic curve, and provides a view of the group complementary to the one here, that will be explained in a forthcoming paper.

References

[1] Y. Dorfman and F. W. Nijhoff. On a $(2+1)$-dimensional version of the Krichever-Novikov equation. *Phys. Lett. A*, 157:107–112, 1991.

[2] W. K. Schief. Lattice geometry of the discrete Darboux, KP, BKP, and CKP equations. Menelaus' and Carnot's theorem. *J. Nonlinear Math. Phys*, 10:194–208, 2003.

[3] A. D. King and W. K. Schief. Tetrahedra, octahedra and cubo-octahedra: integrable geometry of multi-ratios. *J. Phys. A: Math. Gen.*, 36:785–802, 2003.

[4] V. Adler, A. Bobenko, and Y. Suris. Classification of integrable discrete equations of octahedron type. *International Mathematics Research Notices*, 2012, No. 8:1822–1889, 2012. doi: 10.1093/imrn/rnr083.

[5] A. Doliwa. Desargues maps and the Hirota-Miwa equation. *Proc. R. Soc. A*, 466:1177–1200, 2010.

[6] J. Atkinson. On the lattice-geometry and birational group of the six-point multi-ratio equation. *Proc. Royal. Soc. A*, 2014.

[7] V. E. Adler. Some incidence theorems and integrable discrete equations. *Discrete Comput. Geom.*, 36(3):489–498, 2006.

[8] B. G. Konopelchenko and W. K. Schief. Menelaus' theorem, Clifford configurations and inversive geometry of the Schwarzian KP hierarchy. *Journal of Physics A: Mathematical and General*, 35(29):6125, 2002.

[9] A. D. King and W. K. Schief. Clifford lattices and a conformal generalization of Desargues' theorem. *Journal of Geometry and Physics*, 62(5):1088–1096, 2012.

[10] K. Kajiwara, T. Masuda, M. Noumi, Y. Ohta, and Y. Yamada. ${}_{10}E_9$ solution to the elliptic Painlevé equation. *J. Phys. A: Math. Gen.*, 36:L263–L272, 2003.

[11] H. Sakai. Rational surfaces associated with affine root systems and geometry of the painlevé equations. *Communications in Mathematical Physics*, 220(1):165–229, 2001.

[12] A. B. Coble. Points sets and allied Cremona groups (part I). *Transactions of the American Mathematical Society*, 16(2):155–198, 1915.

[13] A. B. Coble. Point sets and allied Cremona groups (part II). *Transactions of the American Mathematical Society*, 17(3):345–385, 1916.

[14] H. S. M. Coxeter. The polytopes with regular-prismatic vertex figures. *Phil. Trans. R. Soc. Lond. A.*, 229:329–425, 1930.

[15] H. S. M. Coxeter. *Regular Polytopes*. Dover books on mathematics. Dover, 1963.

[16] G. R. W. Quispel, J. A. G Roberts, and C. J Thompson. Integrable mappings and soliton equations. *Phys. Lett. A*, 126:419–421, 1988.

[17] M. S. Longuet-Higgens. Clifford's chain and its analogues in relation to the higher polytopes. *Proc. R. Soc. Lond. A.*, 330:443–466, 1972.

[18] W. K. Schief and B. G. Konopelchenko. A novel generalization of Clifford's classical point–circle configuration. Geometric interpretation of the quaternionic discrete Schwarzian Kadomtsev-Petviashvili equation. *Proc. R. Soc. A*, 465:1291–1308, 2009.

[19] S. I. Agafonov. Discrete z^γ: Embedded circle patterns with the square grid combinatorics and discrete Painlevé equations. *Theoretical and Mathematical Physics*, 134:3–13, 2003.

[20] S. I. Agafonov and A. I. Bobenko. Hexagonal circle patterns with constant intersection angles and discrete painlevé and riccati equations. *Journal of Mathematical Physics*, 44:3455–3469, 2003.

[21] A. Doliwa. The affine weyl group symmetry of desargues maps and of the non-commutative hirota–miwa system. *Physics Letters A*, 375(9):1219–1224, 2011.

[22] J. Atkinson. Idempotent biquadratics, Yang-Baxter maps and birational representations of Coxeter groups. *arxiv:1301.4613 [nlin.SI]*, 2013.

[23] J. Atkinson and Y. Yamada. Quadrirational Yang-Baxter maps and the $\tilde{E}_8$ Painlevé lattice. *arXiv:1405.2745 [nlin.SI]*, 2014.